28/38 GHz Antenna for Millimeter Wave 5G Applications with Radiation Pattern Reconfigurability Using CSRR and DGS

Youssef Frist [1, *], Mourad Elhabchi [2], and Mohamed Nabil Srifi [1]

[1] The National School of Applied Sciences, Ibn Tofail University, Kenitra, Morocco
[2] Faculty of Sciences Ben M'Sick, Hassan II University, Casablanca, Morocco
Email: youssefrist@outlook.com (Y.F.); mouradelhabchi@gmail.com (M.E.); srifimn@ieee.org (M.N.S.)
*Corresponding author

***Abstract*—In this research, a novel dual-band antenna is proposed to operate at resonant frequencies of 28 GHz and 38 GHz, which are significant for millimeter-wave 5G applications such as smart cities and the Internet of Things (IoT), utilizing an FR-4 substrate. This study employs a Complementary Split Ring Resonator (CSRR) in conjunction with a Defected Ground Structure (DGS) to achieve dual-band resonant frequencies. This innovative approach enhances key performance metrics, facilitating efficient operation across multiple frequency bands, particularly bandwidth and S11 value. The proposed antenna demonstrates significant improvements, offering an impedance bandwidth of 4.63 GHz and 4.66 GHz for the 28 GHz and 38 GHz bands, respectively. Notably, we obtain an S11 value of −25 dB in the first band (28 GHz) and an S11 value of −70 dB in the second band (38 GHz), demonstrating excellent performance. The directional characteristics of the antenna are evident in the E-plane pattern, focusing the signal in a specific direction. Conversely, the H-plane layout provides omnidirectional coverage, ensuring signal dispersion in all directions. Furthermore, to introduce reconfigurability, Positive Intrinsic Negative (PIN) diodes are integrated to alter the resonant frequencies and radiation pattern direction, enhancing the antenna's adaptability. The design process utilizes Computer Simulation Technology (CST), with validation performed using High Frequency Simulation Software (HFSS) to ensure the accuracy and reliability of the results.**

***Keywords*—dual band, millimeter-wave, 5G applications, Complementary Split Ring Resonator (CSRR), Defected Ground Structure (DGS), reconfigurability, Positive Intrinsic Negative (PIN) diodes**

I. Introduction

In today's technological landscape, individuals' utilization of various applications is continuously increasing, potentially leading to congestion within communication channels. However, attributing the solution solely to 5G technology would be misleading, as it cannot single-handedly meet the escalating demands for data rates and bandwidth imposed by these applications. While 5G undoubtedly brings improvements in these areas, it is not the sole panacea [1]. Additionally, the development of advanced antennas optimized for millimeter-wave (mmWave) frequencies is crucial [2–5]. These antennas enable efficient transmission and reception of signals in the mmWave spectrum, contributing significantly to the enhancement of wireless communication systems. The favored approach no longer leans towards utilizing a solitary antenna element emitting at a specific frequency [6]. Hence, there is a growing need to improve antennas to be reconfigurable. The term" reconfigurable antenna" itself suggests its properties such as frequency agility, and sometimes it can include changes in radiation pattern and even polarization direction according to the application requirements [7, 8]. This adaptability enhances the versatility of antennas, allowing them to dynamically adjust to varying environmental conditions and communication needs. Furthermore, the demand for 5G technology has surged tremendously, leading to an increased demand for antennas operating in millimeter-wave technology [2]. In the literature, numerous researchers have put forth various antenna designs tailored for 5G applications operating within the millimeter-wave spectrum, with particular emphasis on the bands at 28 GHz and 38 GHz [9–11].

The novelty of this work lies in the integration of split ring resonator metamaterial [12–15] and a defected ground structure [16, 17] to enhance the antenna's performance. Additionally, by incorporating reconfigurability functions, this antenna is engineered to be smart, and capable of adapting its functionality dynamically to various operational scenarios. Additionally, the implementation of reconfigurability functions enables the antenna to operate as a multifunctional unit, eliminating the need for multiple antennas. This transformative approach not only enhances performance but also streamlines design complexity, making the antenna a versatile and efficient solution for modern communication systems.

In this study, we introduce a novel dual band antenna design tailored for 5G applications operating within the

Manuscript received May 7, 2024; revised July 19, 2024, accepted August 2, 2024; published September 24, 2024.

millimeter-wave spectrum. Firstly, we present a dual-band microstrip patch antenna inspired by metamaterial and Defected Ground Structure (DGS). This antenna operates efficiently at two resonant frequencies, namely 28 GHz and 38 GHz, both critical for 5G deployment. Secondly, we propose a reconfigurable antenna operating within the same resonant frequencies. This antenna offers versatility by exhibiting different radiation patterns in the E-plane and H-plane. Achieved through the integration of a Positive Intrinsic Negative (PIN) diode, this reconfigurability enables the antenna to spread its coverage in various directions, enhancing its adaptability to diverse communication scenarios.

II. Antenna Configuration

The microstrip patch antenna, depicted in Fig. 1, boasts compact dimensions of 11.8×13.9×1.6 mm^3 and showcases a sophisticated design. Its radiation element, resembling balanced pans inspired by complementary split ring resonator metamaterials, is meticulously crafted from copper with a thickness of 0.035 mm. The ground plane, fashioned in the shape of an inverted T, mirrors this copper construction. Driving its performance is the choice of substrate a 1.6 mm thick FR4 with a permittivity of 4.3 which facilitates efficient signal propagation. The integration of a Defected Ground Structure (DGS) and metamaterials further enhances the antenna's capabilities, elevating its performance to new levels. Specifically, the DGS technique is utilized in this study to expand the impedance bandwidth and refine the radiation pattern. The antenna's parameters, critical for its operation, are calculated using rigorous equations and fine-tuned to meet specific performance criteria outlined in Table I. To validate these results, simulations are conducted using advanced software such as Computer Simulation Technology (CST) Microwave and Ansoft High-Frequency Structure Simulator (HFSS), ensuring accuracy and reliability in real-world applications. Before proposing this structure, we utilized the equations to calculate the dimensions Wp and Lp of the initially proposed antenna depicted in Fig. 2(a). These dimensions were determined based on the formulas provided in reference [18, 19]. This structure yielded two resonant frequencies of 37.76 GHz and 28.54 GHz, with a bandwidth of 14 GHz, as shown in Fig. 3. While these results are promising, our goal is to further enhance the design by incorporating PIN diodes for reconfigurability and achieving multiple resonant frequencies. To this end, we propose adding resonators on the left and right sides of the radiator element of the initial structure by cutting two rectangles, as illustrated in Fig. 2(b). By inserting these two resonators and employing the DGS technique, we aim to achieve the two resonant frequencies for 5G applications: 28 GHz and 38 GHz, as mentioned earlier.

$$W_p = \frac{\vartheta_0}{2f_r}\sqrt{\frac{2}{1+\varepsilon_r}} \tag{1}$$

$$\varepsilon_{reff} = \frac{\varepsilon_r+1}{2} + \frac{\varepsilon_r-1}{2}\left[1+12\frac{h}{W}\right]^{-\frac{1}{2}} \tag{2}$$

$$\frac{\Delta L}{h} = 0.412\frac{(\varepsilon_{reff}+0.3)\left(\frac{W}{h}+0.264\right)}{(\varepsilon_{reff}-0.258)\left(\frac{W}{h}+0.8\right)} \tag{3}$$

$$L_p = \frac{\vartheta_0}{2f\sqrt{\varepsilon_{reff}}} - 2\Delta L \tag{4}$$

$$W_f = \frac{2h}{\pi}\left\{M-1-\ln(2M-1)+\frac{\varepsilon_r-1}{2\varepsilon_r}\left[\ln(M-1)+0.39-\left(\frac{0.61}{\varepsilon_r}\right)\right]\right\} \tag{5}$$

$$M = \frac{377\pi}{2Z_0\sqrt{\epsilon_r}} \tag{6}$$

$$W_s \approx 2\times W_p \tag{7}$$

$$L_s = 2\times L_p \tag{8}$$

The parameters used in the context are:
Wp: radiated patch antenna width,
$\vartheta 0$: speed of light in free space,
$\mathcal{E}_{reff}$: effective relative permittivity,
h: dielectric substrate height,
ΔL: length expansion due to the fringing effect,
Lp: actual radiated patch antenna length,
Wf: width of the feed line,
Ws: substrate width,
Ls: substrate length.

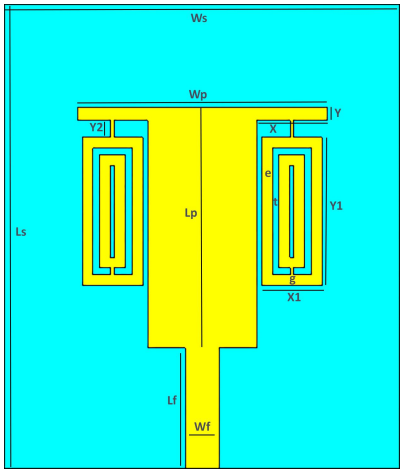

(a)

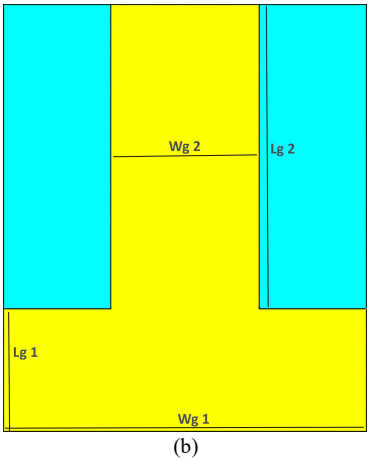

(b)

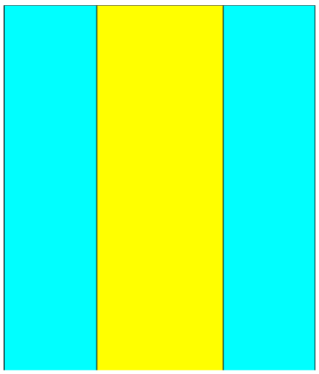

(c)

Fig. 1. The proposed antenna (a) Front view; (b) Optimized partial ground 2 (Proposed), (c) Optimized partial ground 1.

TABLE I. THE DETAILED PARAMETERS OF THE PROPOSED ANTENNA CONFIGURATION

Parameter	Value (mm)	Parameter	Value (mm)
Wp	7.45	Y	0.4
Lp	3	Y2	0.5
Lg1	4	g	0.1
Wg1	11.8	Ws	11.8
e	0.32	Ls	13.9
t	0.2	X1	1.8
Wf	1	Y1	4.45
Lf	3.6	Wg2	.8
X	2.1	Lg2	9.9

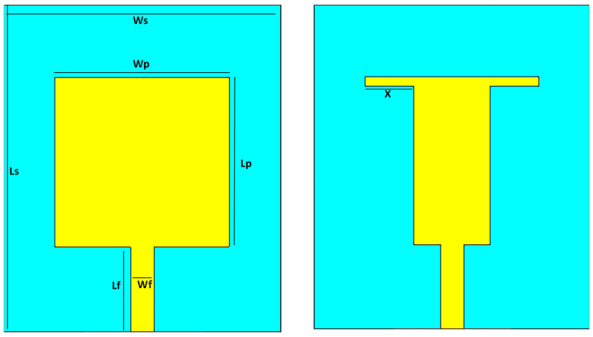

(a) (b)

Fig. 2. Initial structure of the proposed antenna: (a) Step 1; (b) Step 2.

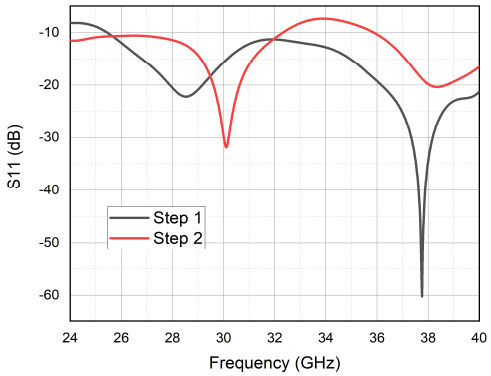

Fig. 3. Initial S11 results for antenna design steps 1 and 2.

III. RESULTS AND DISCUSSION

A. S11 and VSWR

Fig. 4 (a) illustrates the S11 results depicting the evolution in antenna design. It's evident that the antenna functions within the millimeter wave spectrum, particularly in the 24 GHz to 40 GHz range, yielding two resonant frequencies: 28 GHz and 38 GHz, with S11 values of −25 dB and −70 dB respectively. This is accompanied by an expansion in bandwidth within these ranges, attributed to the combined use of metamaterial and Defected Ground Structure (DGS). In the initial iteration, utilizing a full ground, the antenna exhibited two resonant frequencies with enhanced bandwidth, albeit with lower S11 values, especially at the first resonant frequency. Subsequent optimization, seen in Iterations 2 and 3 where partial ground was employed, resulted in a shift toward the desired resonant frequencies of 28 GHz and 38 GHz. These frequencies are sought after for their applicability in 5G technologies. In Fig. 4(b), the Voltage Standing Wave Ratio (VSWR) for the antenna stays below 2 within the two frequency bands, enabling the antenna to operate effectively.

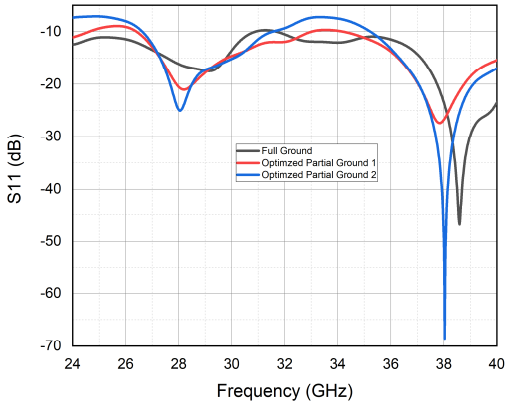

(a)

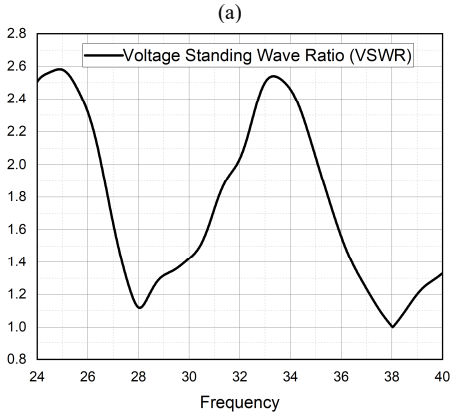

(b)

Fig. 4. The antenna's results of: (a) S11 and (b) VSWR.

B. 3D Gain and Radiation Patterns

In terms of gain, as shown in Fig. 5, the antenna has a positive gain in both frequencies, averaging 2.245 dBi, suggesting that it is useful for signal transmission and reception. This gain is critical for optimizing the antenna's performance in a variety of communication applications. As seen in Fig. 6, the radiation patterns exhibit distinct properties required for antenna deployment. The E-plane pattern exhibits directional behavior by concentrating the signal in a certain direction, which is useful for point-to-point communication or directing signal strength to a

specified target area. In contrast, the H-plane layout provides omnidirectional coverage, evenly spreading the signal in all directions. This omnidirectional feature is useful for applications requiring wide coverage, such as wireless networks or broadcasting systems, as it ensures constant signal reception from multiple directions.

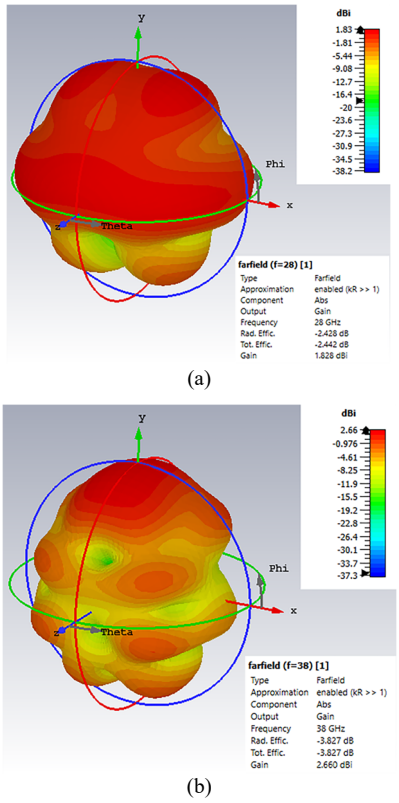

(a)

(b)

Fig. 5. 3D Gain at: (a) 28 GHz and (b) 38 GHz.

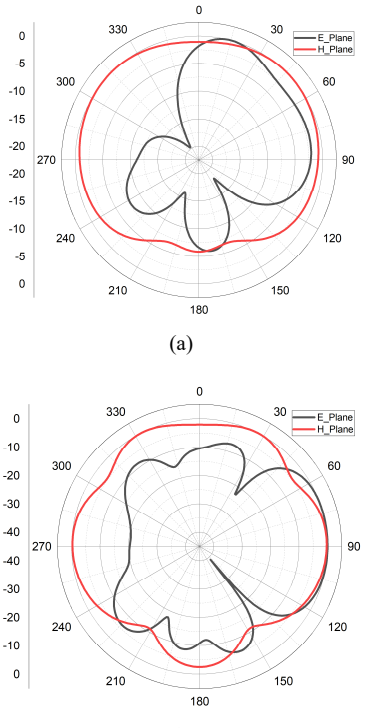

(a)

(b)

Fig. 6. Radiation patterns at: (a) 28 GHz and (b) 38 GHz.

C. *Result of Varying the Antenna Parameters*

In this section, we aim to investigate the effects of altering antenna dimensions, particularly those pertaining to split ring resonators and the ground plane, on the overall performance. In Fig. 7(a), it is observed that varying the distance (t) between the two resonators from 0.2 mm to 0.1 mm with a step size of 0.025 mm does not significantly affect the S11 results, except for the emergence of an intermediate resonant frequency. Conversely, altering the distance (e) has a notable impact on the second band (38 GHz). As depicted in Fig.7(b), increasing the distance from 0.16 mm to 0.32 mm with a step size of 0.04 mm leads to an increase in S11, accompanied by the appearance of an intermediate band exhibiting low S11.When adjusting the width (X1) of the resonator, increasing its value from 1.8 mm to 2 mm with a step size of 0.05 mm results in an enhancement of the S11 within the first band, accompanied by a slight leftward shift. Conversely, there's a decrease in S11 within the second band, also with a slight leftward shift, as illustrated in Fig. 7(c). Regarding the length (Y1) of the resonator, depicted in Fig. 7(d), altering its value from 4.45 mm to 3.35 mm with a step size of 0.225 mm leads to a significant reduction in the S11, along with the appearance of another band exhibiting low S11. Fig. 7(e) and (f) illustrate the variations in the width (Lg2) and length (Wg2) respectively. These variations significantly affect both resonant frequencies in terms of S11 and bandwidth.

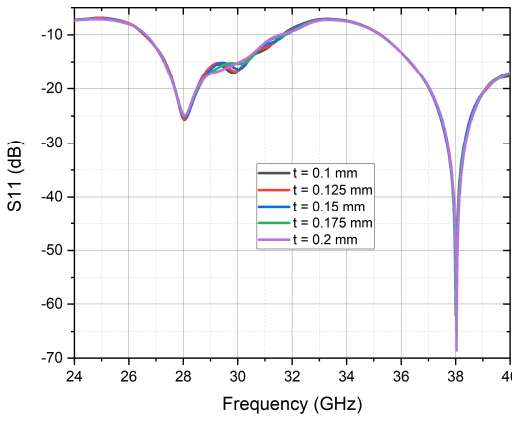

(a)

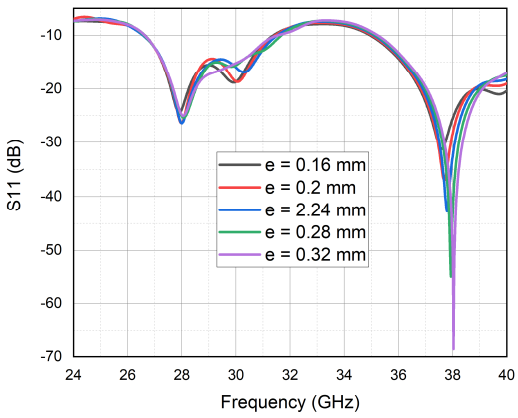

(b)

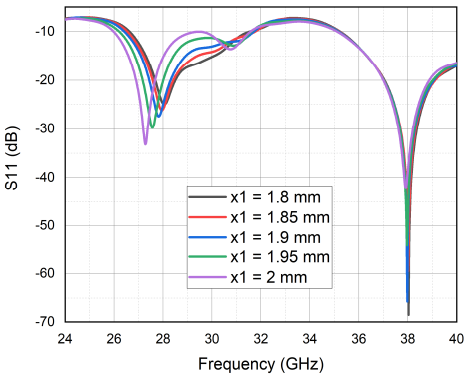

(c)

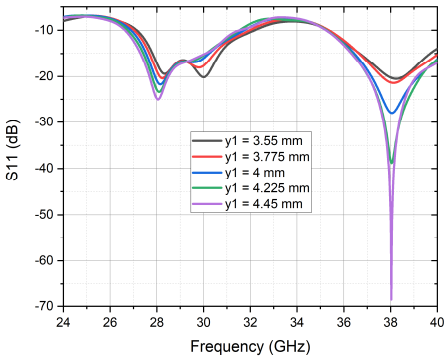

(d)

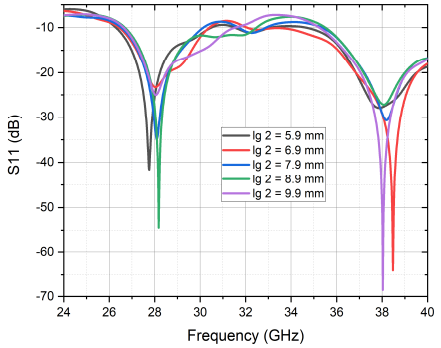

(e)

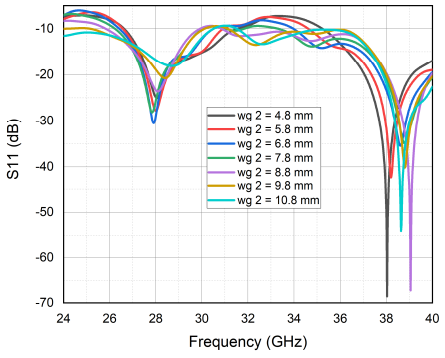

(f)

Fig. 7. Variation of the antenna's parameters.

D. Reconfigurability Function

To achieve additional resonant frequencies and alter the antenna's directional characteristics for frequency and radiation pattern reconfigurability, we implemented a design incorporating split ring resonator metamaterials and a PIN diode, as depicted in Fig. 8(a). The structure of the PIN diode is further elucidated in Fig. 8(b). These PIN diodes were simulated in CST using lumped elements to model their behavior accurately. The equivalent circuit of the PIN diode includes a resistor (Rs), capacitor (CR), and inductor (L) in both the ON and OFF states. In the ON state, Rs is Ω and L is 0.45 nH, while in the OFF state, Rs is 5 MΩ, L remains 0.45nH, and C is 0.14pF. The S11 results, illustrated in Fig. 9, indicate that the PIN diodes predominantly operate within the 28 GHz and 38 GHz bands. Furthermore, the radiation patterns, showcased in Figs. 10 and 11, exhibit a high level of reconfigurability, as detailed in Table II. This table underscores the antenna's capability to adjust both its radiation pattern and resonant frequencies, highlighting its versatility and suitability for various communication scenarios.

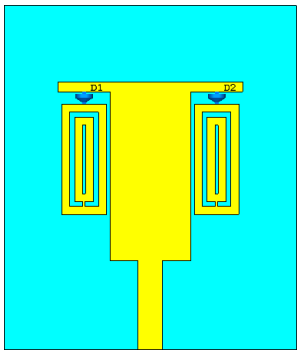

(a)

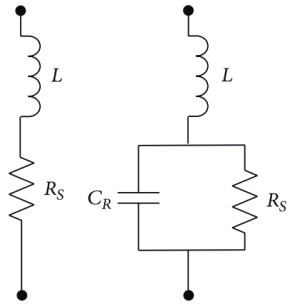

(b)

Fig. 8. Reconfigurability function (a) radiation patterns reconfigurable antenna and (b) Equivalent circuit of the PIN diode.

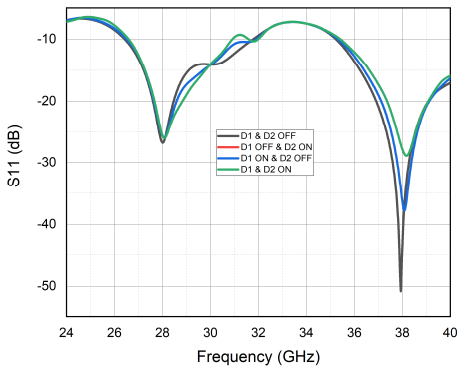

Fig. 9. S11 of the proposed radiation pattern reconfigurable antenna.

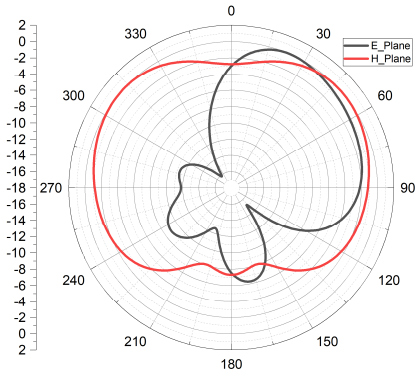

(a)

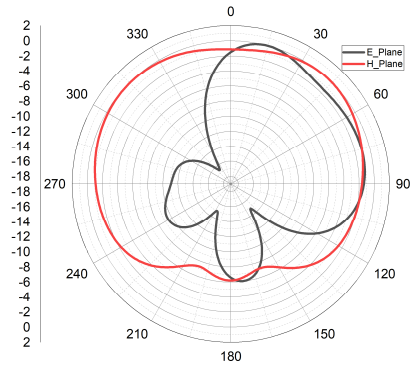

(b)

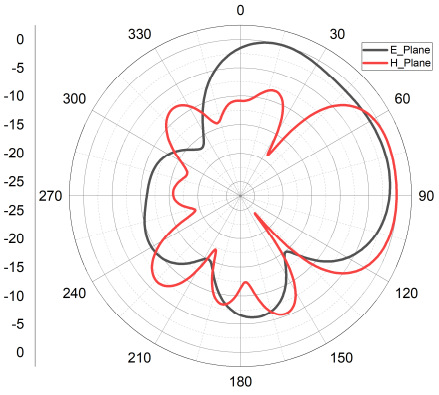

(c)

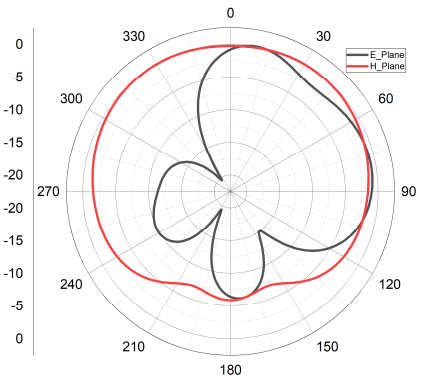

(d)

Fig. 10. E plane and H plane at 28 GHz: (a) D1 and D2 OFF, (b) D1 OFF and D2 On, (c) D1 ON and D2 OFF, (d) D1 and D2 ON.

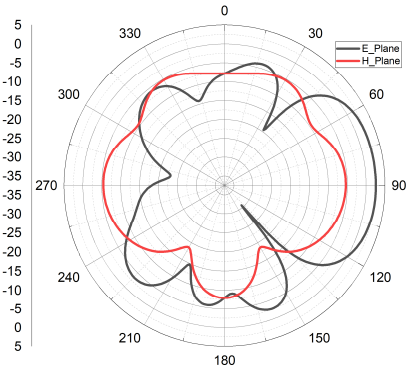

(a)

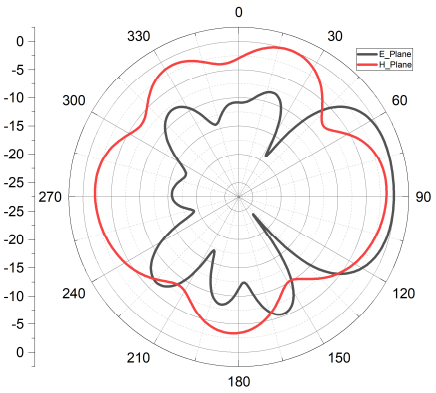

(b)

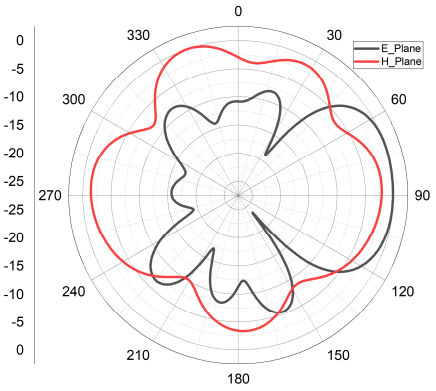

(c)

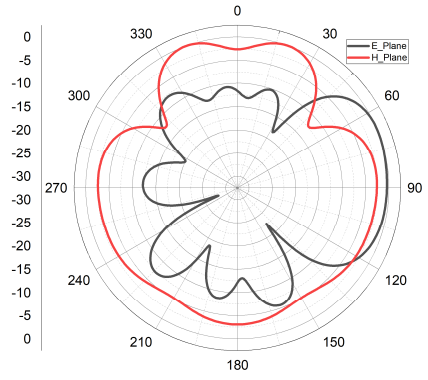

(d)

Fig. 11. E plane and H plane at 38 GHz: (a) D1 and D2 OFF, (b) D1 OFF and D2 On, (c) D1 ON and D2 OFF, (d) D1 and D2 ON.

TABLE II. THE DETAILED PARAMETERS OF THE PROPOSED ANTENNA CONFIGURATION

States		S1	S2	S3	S4
PIN Diodes states	D1	OFF	OFF	ON	ON
	D2	OFF	ON	OFF	ON
Fr (GHz)		28	28.064	28.064	28.096
		37.936	38.08	38.08	38.176
S11 (dB)		−26.70	−25.90	−25.90	−25.95
		−50.22	−37.77	−37.77	−28.89
Gain (dBi)		2.02	2.19	2.19	2.33
		2.55	2.85	2.85	3.26
Beam direction E Plane (deg)		25	15	15	10
		91	72	72	68
Beam direction H Plane (deg)		50	41	41	30
		30	19	19	20

E. Related Work

In this section, we undertake a comprehensive comparison between our proposed antenna and other structures documented in the literature, all operating within the resonant frequencies of 28 GHz and 38 GHz, as detailed in Table III. Our analysis reveals that our proposed antenna not only showcases commendable performance in terms of bandwidth and S11 values but also demonstrates notable advancements in other crucial parameters such as radiation efficiency and gain.

TABLE III. THE DETAILED PARAMETERS OF THE PROPOSED ANTENNA CONFIGURATION

Ref.	Size (mm^3)	Fr (GHz)	BD (GHz)	S11 (dB)	Avg gain (dBi)
[11]	12×11×0.9	38	9.2	−33	9.48
[10]	8×5×0.254	28	3.76	−30	3.12
[1]	15×25×0.508	28/38	0.9; 2	−25; −26	7.45
[4]	7.5×8.8×0.25	28/38	1.23; 1.06	−34.5; −27.3	6.23
[19]	7.14×5.88×0.13	28/29	0.6; 0.5	−34; −29	8.765
This work	11.8×13.9×1.6	28/38	4.63; 4.66	−25; −70	2.245

F. Comparison

To validate our findings, we meticulously recreated the structure within the HFSS software and compared the results with those obtained from CST MWS. The outcomes, depicted in Fig. 12, exhibit a striking similarity in resonant frequency values across both platforms, validating the accuracy of our simulations. These results hold significant implications for millimeter-wave 5G applications, where precise frequency alignment is crucial. Thus, our comprehensive analysis underscores the robustness and reliability of our methodology, strengthening confidence in the suitability of the design for real-world deployment.

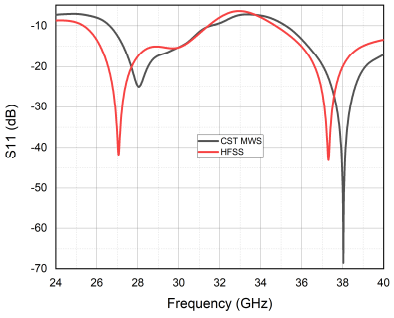

Fig. 12. Comparison of CST MWS and HFSS regarding the S11 results.

IV. CONCLUSION

In conclusion, this work presents a novel dual-band antenna design tailored for millimeter-wave 5G applications, operating specifically at resonant frequencies of 28 GHz and 38 GHz. Through the integration of complementary split ring resonator (CSRR) metamaterial and defected ground structure (DGS), key performance metrics such as bandwidth and S11 value are significantly enhanced. The proposed antenna achieves an impressive impedance bandwidth of 4.63 GHz and 4.66 GHz for the 28 GHz and 38 GHz bands, respectively, with S11 values of -25 dB and -70 dB, demonstrating excellent performance. Moving forward, future work will involve the measurement and characterization of the antenna's performance in real-world environments. This will provide valuable insights into its practical applications and potential optimizations for further enhancement.

CONFLICT OF INTEREST

The authors declare no conflict of interest.

AUTHOR CONTRIBUTIONS

Y.F. Collected and organized data, Wrote the paper; M.E. Conducted the research, and contributed to the interpretation of results; M.N.S. Conceived the research idea, Reviewed and revised the manuscript; all authors had approved the final version.

REFERENCES

[1] P. Liu, X.-W. Zhu, Y. Zhang, X. Wang, C. Yang, and Z. H. Jiang, "Patch antenna loaded with paired shorting pins and h-shaped slot for 28/38 GHz dual-band MIMO applications," *IEEE Access*, vol. 8, pp. 23705–23712, 2020. doi: 10.1109/ACCESS.2020.2964721

[2] G. Kim and S. Kim, "Design and analysis of dual polarized broadband microstrip patch antenna for 5G mmWave antenna module on FR4 substrate," *IEEE Access*, vol. 9, pp. 64306–64316, 2021. doi: 10.1109/ACCESS.2021.3075495

[3] A. Azari, A. Skrivervik, H. Aliakbarian, and R. A. Sadeghzadeh, "A super wideband dual-polarized Vivaldi antenna for 5G mmWave applications," *IEEE Access*, vol. 11, pp. 80761–80768, 2023. doi: 10.1109/ACCESS.2023.3300040

[4] A. E. Farahat and K. F. A. Hussein, "Dual-band (28/38 GHz) wideband MIMO antenna for 5G mobile applications," *IEEE Access*, vol. 10, pp. 32213–32223, 2022. doi: 10.1109/ACCESS.2022.3160724

[5] Y. C. Chang, C. C. Hsu, M. I. Magray, H. Y. Chang, and J.-H. Tarng, "A novel dual-polarized wideband and miniaturized low profile magneto-electric dipole antenna array for mmWave 5G applications," *IEEE Open J. Antennas Propag.*, vol. 2, pp. 326–334, 2021. doi: 10.1109/OJAP.2021.3061961

[6] B. Alekhya, N. A. Murugan, B. T. P. Madhav, and N. Kartheek Ram Reddy, "Millimeter-wave reconfigurable antenna for 5g wireless communications," *Prog. Electromagn. Res. Lett.*, vol. 101, pp. 107–115, 2021. doi: 10.2528/PIERL21070902

[7] J. Hu and Z.-C. Hao, "Design of a frequency and polarization reconfigurable patch antenna with a stable gain," *IEEE Access*, vol. 6, pp. 68169–68175, 2018. doi: 10.1109/ACCESS.2018.2879498

[8] K. Moradi, A. Pourziad, and S. Nikmehr, "A frequency reconfigurable microstrip antenna based on graphene in Terahertz Regime," *Optik*, vol. 228, p. 166201, Feb. 2021. doi: 10.1016/j.ijleo.2020.166201

[9] S. Ashraf, J. A. Sheikh, and Z. A. Bhat, "A high gain multi slotted and compact planar microstrip millimeter wave antenna for 5G networks," *Prog. Electromagn. Res. M*, vol. 108, pp. 175–186, 2022. doi: 10.2528/PIERM22010904

[10] H. Ullah and F. A. Tahir, "A novel snowflake fractal antenna for dual-beam applications in 28 GHz band," *IEEE Access*, vol. 8, pp. 19873–19879, 2020. doi: 10.1109/ACCESS.2020.2968619

[11] I. Shaik and S. Krishna Veni, "Design and analysis of a compact 38 GHz wideband monopole antenna for 5G mm-wave wireless applications," *Prog. Electromagn. Res. C*, vol. 135, pp. 83–94, 2023. doi: 10.2528/PIERC23051902

[12] Y. Frist, M. Elhabchi, and M. Nabil Srifi, "A compact multiband antenna based on metamaterial for L-band, WiMax, C-band, X-band, and Ku-band applications," *TELKOMNIKA Telecommun. Comput. Electron. Control*, vol. 22, no. 1, Oct. 2023. doi: 10.12928/telkomnika.v22i1.25204

[13] C. Feng, T. Shi, and L. Wang, "Novel broadband bow-tie antenna based on complementary split-ring resonators enhanced substrate-integrated waveguide," *IEEE Access*, vol. 7, pp. 12397–12404, 2019. doi: 10.1109/ACCESS.2019.2893881

[14] C. Ni, J. Jiang, W.-J. Wu, L. Zhao, and Z. Fan, "Decoupling method based on Complementary Split Ring Resonator (CSRR) for two cone shipborne antennas," *IEEE Access*, vol. 9, pp. 167845–167854, 2021. doi: 10.1109/ACCESS.2021.3135577

[15] Q. Guo and F. Hao, "Comments on wideband microwave absorber comprising metallic split-ring resonators surrounded with E-shaped fractal metamaterial," *IEEE Access*, vol. 9, pp. 121302–121304, 2021. doi: 10.1109/ACCESS.2021.3108421

[16] G. Chen, C. Guo, J. Xue, Z. Wang, and M. Pang, "Miniaturized metamaterial ultra-wideband antenna for WLAN and Bluetooth applications," *Prog. Electromagn. Res. C*, vol. 132, pp. 117–127, 2023. doi: 10.2528/PIERC23030603

[17] S. Kumar, A. P. Singh, and M. K. Khandelwal, "Theoretical analysis and design of dual band DGS antenna with small frequency ratio for wi-fi and WIMAX applications," *Prog. Electromagn. Res. M*, vol. 62, pp. 153–166, 2017. doi: 10.2528/PIERM17092101

[18] M. Elhabchi, M. N. Srifi, and R. Touahni, "A fractal metamaterial antenna for Bluetooth, WLAN, WiMAX and X-band applications," in *Proc. 2020 International Conference on Intelligent Systems and Computer Vision (ISCV)*, Fez, Morocco, Jun. 2020, pp. 1–5. doi: 10.1109/ISCV49265.2020.9204208

[19] H. M. Marhoon, N. Qasem, N. Basil *et al.*, "Design and simulation of a compact metal-graphene frequency reconfigurable microstrip patch antenna with FSS superstrate for 5G applications," *International Journal on Engineering Applications (IREA)*, vol. 10, no. 3, 193, 2022. doi: 10.15866/irea.v10i3.21752